A Differential Variational Inequality Approach for the Simulation of Heterogeneous Materials

Lei Wang[1], **Jungho Lee**[1], **Mihai Anitescu**[1], **Anter El Azab**[2], **Lois Curfman McInnes**[1], **Todd Munson**[1], **Barry Smith**[1]

[1]Mathematics and Computer Science Division, Argonne National Laboratory, Argonne, IL 60439, USA
[2]Florida State University, Tallahassee, FL 32310, USA

Abstract. The phase-field method has recently emerged as a powerful approach for modeling and predicting mesoscale morphological and microstructure evolution in materials. While differential variational inequalities (DVIs) arise naturally in the phase-field method, the prevailing approach replaces these by smooth approximations that result in equations that are typically very stiff and limit the efficiency and accuracy of the numerical methods applied. This paper discusses initial work in formulating the phase-field equations as a DVI, which is equivalent to a complementarity problem. We solve the system with newly developed nonlinear algebraic solvers for variational inequalities, and we demonstrate that this DVI approach is accurate and efficient for the resolution of heterogeneous materials problems.

1 Introduction

The interactive evolution of grain and interfacial networks is a complex process critical to the long-term performance of heterogeneous materials [11]. In this work, we use a phase-field [5, 10] to model the grain. The phase-field is based on expressing the total free energy functional $\mathcal{E}$ of the heterogeneous material in terms of the free energy of its constituent phases and interfaces. This functional is used to derive kinetic equations for the conserved field variables $(c_1, c_2, ...)$ and non-conserved phase-field variables $(\eta_1, \eta_2, ...)$ of the system [5]

$$\mathcal{E} = \int f(c_1, c_2, ..., c_n, \eta_1, \eta_2, ..., \eta_p) + \sum_{i=1}^{n} \alpha_i (\nabla c_i)^2 + \sum_{i=1}^{3}\sum_{j=1}^{3}\sum_{k=1}^{p} \beta_{ij} \nabla_i \eta_k \nabla_j \eta_k d^3 r \qquad (1)$$
$$+ \int \int G(r - r') d^3 r d^3 r',$$

where f is the local free energy density and α_i and β_i are the gradient energy coefficients. Because the diffuse boundary between phases must be localized, one must use double obstacle potentials for generating the free energy functional. This approach results in a differential variational inequality (DVI). While a comprehensive theory for DVIs has been recently developed [9], the lack of software for large-scale DVIs has led to the situation where the prevailing approach approximates the dynamics of the phase variable by using a smoothed potential, resulting in a stiff problem and undesirable physical artifacts: the phase-field variable does not have compact support, and the boundary between phases of grains in materials is no longer localized. To circumvent these difficulties, we solve the problem in its natural formulation as a DVI.

This paper highlights initial results in solving the system by using scalable nonlinear algebraic VI solvers that leverage and extend the capabilities in PETSc [1] and TAO [4], two libraries of the Towards Optimal Petascale Simulations (TOPS) Center for Enabling Technology.[1]

[1]TOPS website: `http://www.scalablesolvers.org`

2 Mathematical Modeling and Discretization

Without loss of generality, we consider a simplified free energy functional

$$\mathcal{E} = \int \left[f(c,\eta) + \frac{\alpha}{2}(\nabla c)^2 + \frac{\beta}{2}(\nabla \eta)^2 \right] d\Omega, \tag{2}$$

where c is the concentration of a material and η is an order parameter. All analysis can be extended to the general form in (1) in a straightforward manner. Following the standard phase-field approach, the kinetic equations for the spatial and temporal evolution of the concentration field c and the order parameter field η are the modified Cahn-Hillard and Allen-Cahn equations with appropriate boundary conditions,

$$\frac{\partial c}{\partial t} = \nabla \cdot \left(M(c) \nabla \frac{\delta \mathcal{E}}{\delta c} \right) + \xi(\boldsymbol{x}, t), \tag{3}$$

$$\frac{\partial \eta}{\partial t} = -L \frac{\delta \mathcal{E}}{\delta \eta} + \zeta(\boldsymbol{x}, t), \tag{4}$$

where $M(c)$ and L are mobilities and $0 \leq c, \eta \leq 1$. The additional terms in (3) and (4) represent various sources and sinks for the point defect that exist in a material undergoing irradiation damage. We introduce the chemical potential $w = \frac{\delta \mathcal{E}}{\delta c} = \alpha \Delta c + f_c^{'}(c,\eta)$ and rewrite the fourth-order parabolic equation (3) as a system of equations [3] to obtain

$$\frac{\partial c}{\partial t} = \nabla \cdot (M(c) \nabla w) + \xi(\boldsymbol{x}, t). \tag{5}$$

Unfortunately, a naive finite element approximation of the system (4) and (5) does not guarantee that the discrete solution fulfills $0 \leq c, \eta \leq 1$. Therefore, we impose the property $0 \leq c, \eta \leq 1$ as a constraint. This leads to a variational inequality that must be solved at each time step.

We now consider the finite element approximation of equations (4)-(5) under the following assumptions on the meshes. Let Ω be a polyhedral domain and τ^h be a quasi-uniform family of partitionings of Ω into disjoint open simplices κ with $h_\kappa := \mathrm{diam}(\kappa)$ and $h := \max_{\kappa \in \tau^h} \mathrm{h}_\kappa$, so that $\bar{\Omega} = \cup_{\kappa \in \tau^h} \bar{\kappa}$. Associated with τ^h are the finite element space $S^h := \left\{ \chi \in C\left(\bar{\Omega}\right) : \chi|_\kappa \text{ is linear } \forall \kappa \in \tau^{\mathrm{h}} \right\}$ and $K^h := \left\{ \chi \in S^h : 0 \leq \chi \leq 1 \,\mathrm{in}\, \Omega \right\}$. Let Δt denote the time step and $t_n := n\Delta t$. The finite element approximation of equations (4)-(5) is as follows: for $n \geq 1$, find $\boldsymbol{c}^n, \boldsymbol{w}^n, \boldsymbol{\eta}^n \in K^h \times S^h \times K^h$ such that

$$\left(\frac{\boldsymbol{c}^n - \boldsymbol{c}^{n-1}}{\Delta t}, \chi_1 \right) + (M(c^*) \nabla \boldsymbol{w}^n, \nabla \chi_1) + (\boldsymbol{\xi}^*, \chi_1) = 0, \quad \forall \chi_1 \in S^h,$$

$$\alpha \left(\nabla \boldsymbol{c}^n, \nabla(\chi_2 - \boldsymbol{c}^n) \right) + (f_c^{'}(\boldsymbol{c}^*, \boldsymbol{\eta}^*), \chi_2 - \boldsymbol{c}^n) \geq (\boldsymbol{w}^n, \chi_2 - \boldsymbol{c}^n), \quad \forall \chi_2 \in K^h,$$

$$\left(\frac{\boldsymbol{\eta}^n - \boldsymbol{\eta}^{n-1}}{\Delta t}, \chi_3 - \boldsymbol{\eta}^n \right) + L \left(\beta \nabla \boldsymbol{\eta}^n, \nabla(\chi_3 - \boldsymbol{\eta}^n) \right) + L(f_\eta^{'}(\boldsymbol{c}^*, \boldsymbol{\eta}^*), \chi_3 - \boldsymbol{\eta}^n) + (\boldsymbol{\zeta}^*, \chi_3) \geq 0,$$
$$\forall \chi_3 \in K^h,$$

where $(\cdot)^* = (\cdot)^n$ or $(\cdot)^{n-1}$ and $\boldsymbol{c} = \sum_{i=1}^N c(x_i)\phi_i, \boldsymbol{w} = \sum_{i=1}^N w(x_i)\phi_i, \boldsymbol{\eta} = \sum_{i=1}^N \eta(x_i)\phi_i$ are finite-dimensional approximations with $\{\phi\}_{i=1}^N$ being the standard Lagrange "hat" basis functions. We have a complementarity formulation [6] of the coupled Cahn-Hillard and Allen-Cahn

equations (4)-(5):

$$0 = M_0 \frac{\boldsymbol{c}^n - \boldsymbol{c}^{n-1}}{\Delta t} + M_1 \boldsymbol{w}^n + M_0 \boldsymbol{\xi}^*, \tag{6}$$

$$0 = \alpha M_2 \boldsymbol{c}^n + M_0 f_c^{'}(\boldsymbol{c}^*, \boldsymbol{\eta}^*) - M_0 \boldsymbol{\omega}^n + \boldsymbol{\lambda}_1 - \boldsymbol{\mu}_1 \tag{7}$$

$$0 = M_0 \frac{\boldsymbol{\eta}^n - \boldsymbol{\eta}^{n-1}}{\Delta t} + L\beta M_2 \boldsymbol{\eta}^n + L M_0 f_\eta^{'}(\boldsymbol{c}^*, \boldsymbol{\eta}^*) + M_0 \boldsymbol{\zeta}^* + \boldsymbol{\lambda}_2 - \boldsymbol{\mu}_2 \tag{8}$$

$$0 \le \boldsymbol{\lambda}_1 \perp 1 - \boldsymbol{c}^n \ge 0, \quad 0 \le \boldsymbol{\mu}_1 \perp \boldsymbol{c}^n \ge 0, \tag{9}$$

$$0 \le \boldsymbol{\lambda}_2 \perp 1 - \boldsymbol{\eta}^n \ge 0, \quad 0 \le \boldsymbol{\mu}_2 \perp \boldsymbol{\eta}^n \ge 0, \tag{10}$$

where $M_{0i,j} = (\phi_i, 1)_{L^2(\Omega)}$, $M_{1i,j} = (M(c^*(x_i))\nabla\phi_i, \nabla\phi_j)_{L^2(\Omega)}$, and $M_{2i,j} = (\nabla\phi_i, \nabla\phi_j)_{L^2(\Omega)}$ and $\boldsymbol{\lambda}_{1,2}, \boldsymbol{\mu}_{1,2} \in \mathbb{R}^N$ are Lagrange multipliers. We then can use parallel solvers for complementarity problems in PETSc and TAO.

3 Algorithms and Software

To solve the algebraic DVIs that arise at each timestep of these mesoscale simulations, we are investigating algorithms developed by the optimization community for solving complementary problems based on formulating them as nonsmooth systems of equations. We have already implemented two parallel nonlinear algebraic VI solvers in the PETSc library: a semi-smooth algorithm and a reduced-space active set algorithm. To solve the resulting linear systems, we are exploring a multigrid method with block Gauss-Seidel smoothing [2] and Schur complement preconditioners that incorporate a multigrid (either algebraic or geometric) solver.

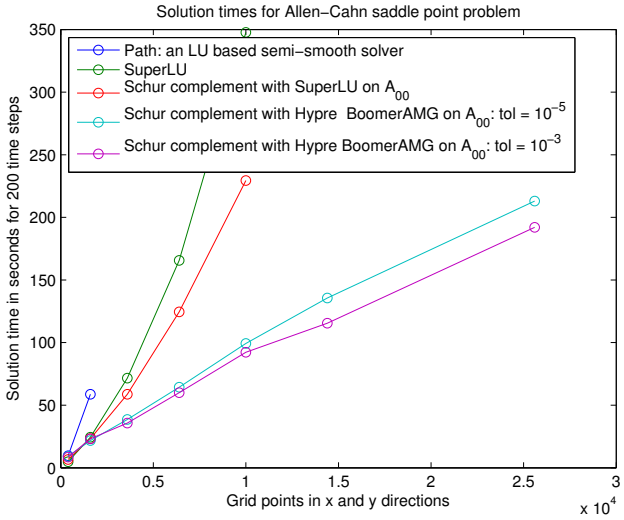

Figure 1: Solution times for an Allen-Cahn saddle point problem; we demonstrate mesh-independent convergence rates for the Schur complement preconditioner that incorporates algebraic multigrid.

We have completed preliminary numerical experiments and mathematical analysis for the Allen-Cahn system that demonstrate mesh-independent convergence rates for the Schur complement preconditioner. That is, the work required to solve a single timestep grows linearly with the number of unknowns. In Figure 1 we plot the time to solution for 200 timesteps using

several solver approaches for the Allen-Cahn model in two dimensions. For the innermost solve in the Schur complement we leverage complementary TOPS capabilities by employing PETSc's interface to LLNL's BoomerAMG algebraic multigrid solver in the hypre library.

4 Numerical Experiments

The DVI approach is now demonstrated by solving the problem of void growth under irradiation. The corresponding model has two concentration fields for the point defects, vacancies c_v and interstitials c_i, and one phase field demarcating the void and matrix region. This model is introduced in [7]. We omit the detailed description here because of limited space.

Some preliminary computational results are shown in Figure 2. The upper row shows the case of void growth in a supersaturated vacancy field. The void grows as a result of the absorption of vacancies from the adjacent solid regions. The interstitial concentration in the solid remains at equilibrium throughout the time. Within the void, the values of the concentration and order parameter fields are $c_v = 1$ and $c_i = 0$, respectively, throughout the evolution. The lower row shows the void shrinks that occur as a result of the recombination of interstitials with vacancies at the void surface. These numerical results agree with those presented in [7]. One of the benefits of our DVI approach is that the numerical solutions c_v and η by design lie in the interval $[0, 1]$ and do not need any clamping.

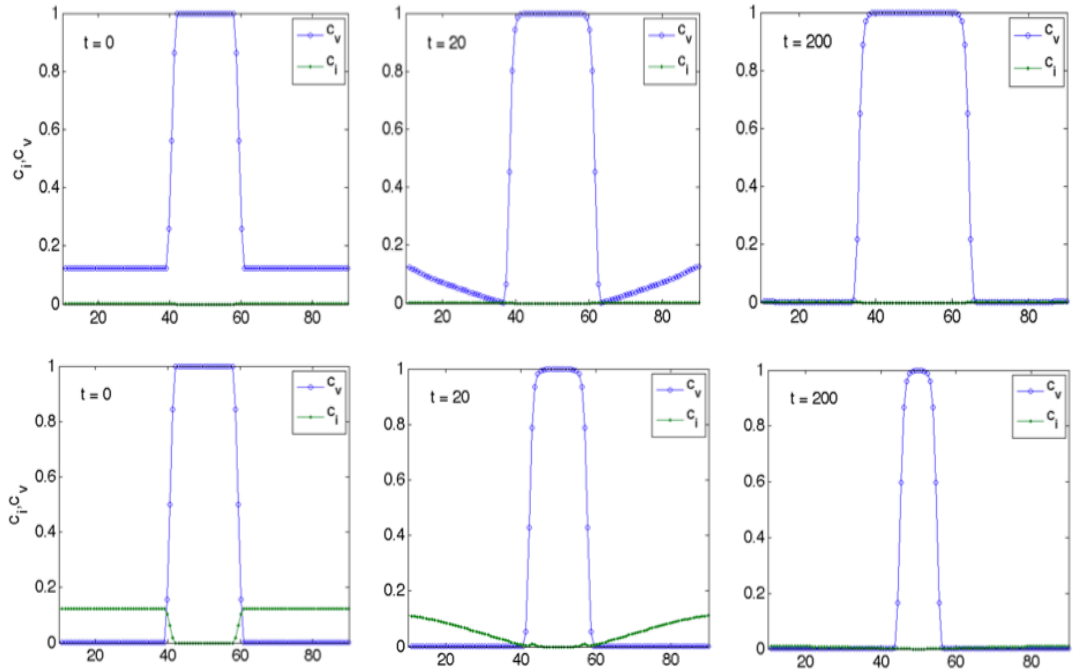

Figure 2: Plots of the concentration fields c_v and c_i throughout the time. Upper row: the void grows due to the absorption of vacancies from the adjacent solid regions. Lower row: the void shrinks due to the recombination of interstitials with vacancies at the void surface.

5 Summary

We use the coupled Cahn-Hilliard and Allen-Cahn systems with a double-obstacle free energy potential to simulate heterogeneous materials problems. A naive finite element approximation does not guarantee that the discrete solution satisfies appropriate constraints. Therefore we formulate a DVI, which is equivalent to a complementarity problem. This approach allows us to use parallel solvers for complementarity problems in PETSc and TAO. We have validated the DVI approach against the baseline results in [7], and we are extending to address additional models discussed in [8] as well as to explore issues in scalable VI algorithms and software.

Acknowledgments. This work was supported by the Office of Advanced Scientific Computing Research, Office of Science, U.S. Department of Energy, under Contract DE-AC02-06CH11357. A. El Azab is supported by the Energy Frontier Research Center on Materials Science of Nuclear Fuel, funded by the U.S. Department of Energy, Office of Basic Energy Sciences under subcontract number 00091538 at Florida State University.

References

[1] S. Balay, K. Buschelman, V. Eijkhout, W. Gropp, D. Kaushik, M. Knepley, L. McInnes, B. Smith, and H. Zhang, "PETSc Users Manual," Tech. Rep. ANL-95-11-Revision 3.1, Argonne National Laboratory, 2010, see `http://www.mcs.anl.gov/petsc`.

[2] L. Baňas and R. Nürnberg, "A Multigrid Method for the Cahn-Hilliard Equation with Obstacle Potential," Applied Mathematics and Computation (213), no. 2, pp. 290–303, 2009.

[3] J. Barrett, J. Blowey and H. Garcke, "Finite Element Approximation of the Cahn-Hillard Equation with Degenerate Mobility," SIAM J. Numer. Anal. (37), pp. 286-318, 1999.

[4] S. Benson, L. C. McInnes, J. Moré, T. Munson, and J. Sarich, "Toolkit for Advanced Optimization (TAO) Users Manual," Tech. Rep. ANL/MCS-TM242 - Revision 1.10.1, Argonne National Laboratory, 2010, see `http://www.mcs.anl.gov/tao`.

[5] L. Chen, "Phase-field Models for Microstructure Evolution," Annual Review of Materials Research (32), pp. 113-140, 2002.

[6] D. Kinderlehrer and G. Stampacchia, *An Introduction to Variational Inequalities and Their Applications*, Philadelphia: Society for Industrial Mathematics, 2000.

[7] P. Millett, A. EI-Azab, S. Rokkam, M. Tonks and D. Wolf, "Phase-field Simulation of Irradiated Metals, Part I: Void Kinetics," Comp. Mate. Sci. (50), pp. 949–959, 2011.

[8] P. Millett, A. EI-Azab and D. Wolf, "Phase-field Simulation of Irradiated Metals, Part II: Gas Bubble Kinetics," Comp. Mate. Sci. (50), pp. 960–970, 2011.

[9] J.-S. Pang and D. E. Stewart, "Differential Variational Inequalities," Mathematical Programming, (113), no. 2, pp. 345-424, 2008.

[10] K. Thornton, J. Agren and P. Voorhees, "Modeling the Evolution of Phase Boundaries in Solids at the Meso- and Nano-scales," Annual Review of Materials Research (32), pp. 113-140, 2002.

[11] S. Yip, *Handbook of Materials Modeling*, Springer, 2005.